The Effect of the January 10, 1997 Pressure Pulse on the Magnetosphere-Ionosphere Current System

E. Zesta[1], H. J. Singer[2], D. Lummerzheim[3], C. T. Russell[4], L. R. Lyons[1], M. J. Brittnacher[5]

---

[1] Department of Atmospheric Sciences, University of California Los Angeles, Los Angeles, CA 90095-1565

[2] Space Environment Center, National Oceanic and Atmospheric Administration, Boulder, CO, 80303

[3] Geophysical Institute, University of Alaska, Fairbanks, AK 99775

[4] Institute of Geophysics and Planetary Physics, UCLA, Los Angeles, CA 90095

[5] Geophysics Program, University of Washington, Seattle, WA, 98195

On January 10, 1997 a strong pressure pulse, observed by the WIND spacecraft between 1030 and 1055 UT, hit the magnetosphere, after about a one-half hour delay, causing the strengthening and widening of the auroral electrojet at all local times. The duration of the electrojet perturbation was the same as the duration of the solar wind pressure pulse. The pulse occurred during the well-studied Jan 10-11, 1997 magnetic storm and during strong geomagnetic activity. We study the effect of the pressure pulse on the ionospheric current, using a global network of more than 100 ground magnetometers, images from the POLAR spacecraft, and solar wind measurements from the WIND and Geotail spacecraft. We find that the magnetospheric and ionospheric response is directly driven by the solar wind conditions and clearly related to the onset, duration and end of the pressure pulse. In addition it appears that the enhancement of the Region 1 currents opposed the effect of the enhancement of the magnetopause current for locations near noon. These responses are not characteristics of a typical substorm.

INTRODUCTION

The response of Earth's magnetosphere to solar wind pressure enhancements has been studied primarily for interplanetary shocks and sudden pressure increases. Sudden Impulses (SI) and Storm Sudden Commencements (SSC) are due to solar wind pressure enhancements usually associated with interplanetary shocks, the latter accompanied by a magnetic storm event. The effect of SI and SSC events has been studied by Araki [1977, 1994], and for both northward and southward IMF by Russell et al. [1994a, 1994b] and others. Sudden enhancements in the solar wind dynamic pressure are known to compress the magnetosphere and enhance the magnetopause current (Kauffman and Konradi, 1969), as well as the tail currents (Russell et al., 1994a). The response can be very different for northward and southward IMF. For northward IMF, the magnetic field observed at low, mid- and sub-auroral latitudes, ≤55° geomagnetic, responds with a positive perturbation in the H component due primarily to the increased magnetopause current (Araki, 1994, and references therein, Russell et al., 1994a, Le et al., 1993, Russell and Ginskey, 1995). At geomagnetic latitudes greater than 60°, the response is due primarily to increased Region 1 currents that result from the magnetospheric compression. Russell et al. [1994b] showed that for SI events during southward IMF the response of the dayside sub-auroral latitudes to the magnetopause currents is significantly reduced by the enhanced Region 1 currents that result from increased dayside reconnection.

The Jan 10-11, 1997 magnetic cloud event, and the magnetic storm resulting from it, is a well-documented event with extensive data coverage. There were two substorm events, at about 0337 and 0645 UT (Li et al., 1998), before the pressure pulse hit the magnetosphere, followed by steady southward IMF and a continuous increase in geomagnetic activity between 0730 and 1030 UT. Shue and Kamide [1998] studied the correlation between the solar wind dynamic pressure and the strength of the westward electrojet, mostly in the vicinity of local midnight, for the 0 to 12 UT time period on Jan 10, 1997. They concluded that the solar wind density strongly affects the strength of the westward electrojet when the IMF has been southward for some time, but the coupling is weak for northward IMF. Kamide et al. [1998] examined the same pressure pulse that we examine here and argued that there were two substorm onsets, the first at around 1035 UT, internally triggered, and a second around 1050 UT triggered by the solar wind dynamic pressure pulse. Both Shue and Kamide [1998] and Kamide et al. [1998] interpret the influence of the solar wind dynamic pressure on the magnetosphere in terms of substorm triggering. There are several studies that suggest that substorms can be triggered by SSC events when the IMF is southward [Burch, 1972, Iijima, 1973, and Kokubun et al., 1977].

In the present paper we analyze the effect of the Jan 10, 1997 pressure pulse. We find an auroral enhancement at ~1035 UT, likely a substorm onset, preceding the pressure pulse; but we see no clear evidence for a typical substorm triggered by the pressure pulse. Rather the effects of the pulse are intense and global with a rapid response at all local times simultaneously. These include a dramatic increase of the morning-side westward auroral electrojet, during all local times from 00 to 12 MLT, and the poleward expansion and widening of the auroral oval. We should clarify here that in our use of the term “auroral westward electrojet” we refer to the global ionospheric electrojet associated with the morning convection cell (the global electrojet is westward in the morning sector and eastward in the afternoon) as opposed to the substorm westward electrojet, that is localized around 0 MLT and is associated with auroral surges and the substorm current wedge. The increase of the auroral electrojet during the pressure pulse event implies the global and dramatic increase of the Region 1 currents (see Siscoe et al., 1991 for a description of the circuit that connects the boundary layer, the R1 currents and the ionospheric currents). The poleward expansion of the auroral oval implies significant increase in closed flux in the magnetotail.

THE PRESSURE PULSE IN THE SOLAR WIND

The pressure pulse examined herein was observed by the WIND spacecraft between 1030 and 1055 UT and is shown in Figure 1. At the time WIND was located at GSE (88.5,-58.6,-3.9) R_E. From top to bottom, Figure 1 shows the solar wind bulk velocity, proton density, thermal speed, total magnetic field strength, and the B_x, B_y, B_z magnetic field components in the GSM coordinate system. The two vertical lines at 1030 and 1055 UT indicate the duration of the solar wind density pulse. The speed is steady at 445 km/s. The dynamic pressure pulse then is entirely due to the density pulse. The IMF remains strongly southward at about –10 nT with a strong negative B_y component and it is slowly rotating northward. There is a small disturbance in B_z and B_y, lasting only a couple of minutes and with a magnitude less than 2 nT, associated with the onset of the pressure pulse, but there are no major magnetic perturbations associated with the pulse. The sum of the perpendicular thermal and magnetic pressure is constant across the discontinuity and the velocity is constant. These are the properties of a tangential discontinuity [Burgess, 1995]. This non-propagating (in the solar wind frame) density structure causes a dynamic pressure pulse when it encounters the magnetosphere.

Figure 2 shows the plasma and magnetic field data from the Geotail spacecraft, which was at GSE (6.3,9.3,0.5) R_E during this period and mostly within the afternoon magnetosheath. Geotail observes the same density pulse that WIND observes with a similar rise and decay and 25 minute duration, shown between the two dashed lines in the Figure 2. The onset of the pulse at Geotail is at 1053 UT, 23 minutes later than WIND. From the magnetic field data we deduce that Geotail was continuously in the magnetosheath from 0950 until 1113 UT, when it crossed the magnetopause boundary. The dotted vertical lines indicate transitions from the magnetosphere to the magnetosheath and back. The two bars on the top of the figure indicate the time periods that Geotail was in the magnetosphere. The crossing of the boundary at 1113 UT coincides with the sharp drop of the pressure pulse, implying that the magnetopause expanded beyond the position of Geotail as the magnetosphere relaxed after being compressed by the pulse.

We determine the size and orientation of the solar wind structure associated with the pressure pulse in order to accurately determine its effect on the magnetosphere. By comparing the magnetic and thermal pressure in the structure we find that it is in thermal balance in the frame of reference of the moving plasma. Specifically, the total pressure was 8.58×10^{-2} nPa before the pressure pulse, and 8.24×10^{-2} nPa during the pressure pulse. This is only a 4% change. Both the total magnetic field, B_t, and the thermal speed (and therefore the plasma temperature), decrease slightly during the pressure pulse to balance the strong increase in density (see Figure 1). Such a structure would more than likely be a tangential discontinuity aligned with the magnetic field and more than likely cylindrical with its axis along the IMF. If this were a rotational discontinuity, which could propagate with a normal at an oblique angle to the field, the density would be constant across the surface (e.g. Burgess, 1995), and this is not the case here. For a tangential discontinuity aligned with the IMF, the diameter of the cylinder should be at least 89 R_E, which is the distance determined by the duration of the pressure pulse projected in the direction perpendicular to the IMF. We also know that the length of the cylinder is at least 84 R_E, which is the Y separation of WIND and Geotail projected along the IMF. Therefore the solar wind structure would be at least 89 RE in the X-direction and 84 RE in the Y-direction and therefore large enough that when it encounters the magnetosphere it engulfs it all from the dayside to the far nightside. The above analysis also implies that we can be certain that when the pressure pulse is observed by Geotail at 1053 UT, it should also encounter the magnetopause at approximately the same time.

THE MAGNETOSPHERIC AND IONOSPHERIC RESPONSE

We investigate the magnetospheric and ionospheric response by examining the aurora observed by the UVI instrument on Polar (Torr et al., 1995), and by inferring the equivalent ionospheric current patterns from a global network of ground magnetometers.

Plate 1 shows a series of 25 auroral images, from 1020 to 1130 UT, observed with the POLAR UVI imager. Each image shows the two-dimensional distribution of the precipitating particle energy flux in a MLT – magnetic latitude coordinate system. The UVI instrument has several filters. We used images taken with the LBH-long filter. The brightness of the images in this passband is proportional to the incident energy. Each image is calibrated and pixels are binned into a regular grid (1° by 10°) in latitude-longitude geomagnetic coordinates. The energy flux is then obtained from a parameterization of the image brightness based on the Lummerzheim and Lilensten [1994] auroral model. Between 1000 and 1030 UT there is moderate auroral activity extending from the evening side to beyond midnight. Between 1035 and 1040 UT there is a strong auroral enhancement around 24 MLT that by 1047 UT spreads towards both dusk and dawn and becomes a global enhancement, at 63° geomagnetic latitude. Kamide et al. [1998] identified this auroral enhancement at 1035 UT from ground magnetometers and auroral images as a substorm onset. Li et al. [1998] (their Figure 4) identified a particle injection at geosynchronous around 1035 UT. This intensification occurs more than 15 minutes before the pressure pulse hits the magnetosphere and is therefore unrelated to it. Kamide et al. also argue that there is a second substorm onset that is triggered by the pressure pulse. In our analysis the series of images in Plate 1 are consistent with a continuous strengthening of the aurora from 1050 UT onwards, rather than a clear second substorm onset.

The first signatures of the pressure pulse arriving at the magnetopause are seen shortly after 1050 UT, possibly 1-2 minutes earlier than at Geotail, due to the orthospiral orientation of the IMF and Geotail's location in the afternoon region. The image at 1050:45 UT shows a widening of the auroral oval as it continues to intensify. Until 1048 UT the oval extends from 55°to 71° geomagnetic latitude, while at 1050:45 UT it extends for the first time poleward of 71°. We believe this is the response of the magnetosphere to the initial compression as the pressure front hits the magnetopause boundary, resulting in an increase of the dayside magnetic field and the Chapman-Ferraro current. As a consequence, the Region 1 current circuit also strengthens. Around 1056:53 UT the poleward expansion of the oval accelerates. From 1047:41 UT to 1053:49 UT, a ~6-minute interval, the poleward boundary of the oval moved very little and remained at ~71°. However between 1054:26 and 1100:34 UT, another 6-minute interval, the poleward boundary moves from 71° to 78°. As can be seen from Figure 2, this corresponds to the time when the solar wind density at the dayside magnetopause began to increase at a faster rate. The poleward expansion of the auroral oval ended near 1103 UT, very soon after the time that the peak solar wind density hit the magnetopause. The 1106:05 UT image in Plate 1 shows the oval extending to almost 80° geomagnetic latitude, implying that a significant amount of nightside magnetic flux in the lobes has become closed. The continuous poleward expansion of the auroral oval from 1050 to 1103 UT suggests a continuous increase in nightside reconnection. Auroral intensities start to decrease at ~1103 UT and seem to follow the decrease in the solar wind density. By 1121:25 UT, seven minutes later, the intensity is dramatically decreased and the poleward boundary of the oval starts to move back to lower latitudes. By this time the end of the pressure enhancement region in the solar wind has reached far downtail. These observations show a very fast and direct response of the magnetosphere to the phases of the pressure pulse and therefore we interpret the intensification not as a new onset but as a directly driven response of the magnetosphere to the pressure pulse affecting ongoing activity. Similar conclusions have been reached using observations from the POLAR VIS camera (John Sigwarth, personal communication).

The bottom panel in Plate 1 shows the 5577Å-emission line from the meridional scanning photometers (MSP) from Rankin Inlet and Gillam. The two stations are located at the same MLT, separated only in latitude, so the data from the two stations are merged to increase the latitudinal coverage. The stations are located at 0430 MLT during the pressure pulse event. The data show very clearly the widening and strengthening of the auroral oval between 1050 and 1115 UT, exactly the duration of the pressure pulse that encounters the magnetosphere. The top white line in the keogram identifies the separatrix boundary to within 2° (Blanchard et al, 1997). This is yet another indication for the directly driven response of the magnetosphere/ionosphere to the pressure pulse.

Figure 3 complements the Plate 1 images and is a representative sample of the interpolated global equivalent ionospheric current patterns determined from the global network of magnetometers. The currents are plotted in an MLT – magnetic latitude coordinate system. The locations of the ground magnetometers are marked with solid triangles. Magnetic local noon is at the top of each dial and the UT time is indicated at the top right corner. The stations create an irregular grid of data points; therefore we applied a spherical interpolation technique to produce the two-dimensional equivalent ionospheric current patterns in a 10° by 1° longitude-latitude grid. To convert the magnetic perturbations in nT to height-integrated ionospheric current in A/m we used the conversion scale of 500 nT per A/m total ionospheric current, based on the measured geomagnetic effects of the Hall and Pedersen currents by Araki et al. [1989]. It should be noted that the Araki et al. [1989] conversion scale is accurate only under the well-developed auroral electrojets, in our case between latitudes 65° and 75°. Beyond those latitudes the approximation may not work as well. We corrected for the ground-induced currents by multiplying the equivalent current by a factor of 2/3. The current at the edges of our grid should be ignored, because of large edge effects, in particular the region around 0 MLT and at latitudes less than 60°.

At 1030 UT the morning convection cell is seen with the auroral westward electrojet located between 60° and 70° at local times from 0 to 13 MLT. At 1040 UT a small strengthening of the electrojet, localized in the midnight region, coincides with the strengthening in the auroral images in Plate 1. At 1050 UT, when the pressure pulse hits the magnetosphere, we see the first indication of a far more global strengthening of the ionospheric current system. By 1055 UT the region of significant current has widened, now located between 75° and 60° geomagnetic latitude, and reaching more than 3 A/m. During the next 15 minutes the auroral electrojet extends from 50° to 80° in excellent agreement with the very wide oval observed in the auroral images in Plate 1. The strengthening and widening of the ionospheric current system is indirect evidence for the significant strengthening of the Region 1 field-aligned currents (e.g. Siscoe et al., 1991). Previously this has been indirectly inferred by Russell et al. [1994b], who found that the dayside response to the SI compression, namely the increase of the magnetopause current, is more than 25% smaller when the IMF is southward than when it is northward. They attribute this to the increase of the Region 1 currents associated with increased dayside reconnection.

Further evidence for the driven effect of the pressure pulse on the magnetosphere is shown in Figure 4. The H component from ground magnetometers covering 0 to 13 MLT are plotted for stations at greater than 70° geomagnetic latitude in the left panel, stations with latitudes between 60° and 70° in the middle panel, and stations with latitudes between 50° and 60° in the right panel. The vertical line in all three panels indicates the time that Geotail observed the onset of the pressure pulse, 1053 UT. All the stations at higher than 70° latitude, except for Contwoyto, observe a large negative bay starting around 1050 UT (Contwoyto observes a strengthening of a pre-existing bay at that time). These stations are poleward of the auroral oval before the pressure pulse (see Plate 1) and observe the transient strengthening and widening of the westward auroral electrojet between 1050 and 1120 UT. All these stations (except Sachs Harbour) show the onset of a strong reduction in bay intensity at 1115 UT, the time of the end of the pressure pulse. The auroral stations in the middle panel also see the negative bay after 1050 UT, except for Kilpisjarvi that sees the strengthening of the afternoon eastward electrojet. The stations closer to 0 MLT however, College and Fort McMurray, observe the prior substorm intensification between 1035 and 1050 UT. The sub-auroral stations in panel 3 observe more complicated signatures. Some observe both the substorm and the pressure pulse effect (Glenlea, Ottawa) and others only the pressure pulse (Newport, Saint John, Nurmijarvi).

In summary, it is evident from Figures 3, 4, and 5 that the response of the magnetosphere to the pressure pulse is almost instantaneous and global, and appears to be directly driven by the impact and propagation of the pressure pulse in the magnetosphere. We observe a possible substorm onset between 1035 and 1040 UT, also described by Kamide et al. [1998], that occurs before the pressure pulse arrives at the magnetosphere. The initial response to the compression, occurring around 1050 UT, is the strengthening of the Region 1 currents evidenced by the global strengthening of the electrojet (Siscoe et al., 1991). About 7 minutes later, and for the next 15 minutes, we observe a significant increase in the closed flux in the tail indicated by the broadening of the electrojet and the auroral oval. The increase in closed flux implies that the pressure pulse caused an enhancement in nightside reconnection.

COMPARISON WITH TYPICAL SUDDEN IMPULSE EVENTS

The response of the magnetosphere to pressure increases associated with shocks, SI and SSC events, has been investigated for all latitudes and both northward and southward IMF conditions (Araki [1977, 1994], Russell et al [1994a, 1994b], Le et al. [1993], Russell and Ginskey [1995] and others). The general consensus is that SI events have a sharp signature at all latitudes, but at the dayside sub-auroral mid and low latitudes the ground magnetometers all observe a positive main signature in the H component, as a direct response to the increased Chapman-Ferraro current at the magnetopause.

Figure 5, panel (a), is a stack plot of the H component of eight stations in the 10 to 13 MLT region ranging in magnetic latitude from 52° to -42°. Stations as low as 42° (L=1.5) show a negative bay instead of the customary positive deflection. All these stations respond to the very strong auroral westward electrojet and the Region 1 currents that cancel out and overshoot the effect of the increased Chapman-Ferraro current. It is only at latitudes lower than 40° that we see the response to the magnetopause current. Panel (b) of Figure 5 shows the response of mid to low latitude stations at all MLT locations. The magnetic latitude and exact MLT location for each station is indicated on the plot. Notice that locations away from local noon show the response to the increased magnetopause current at mid-latitudes around 40° geomagnetic, e.g. Boulder, Canberra. It is only at the region a few hours around local noon that the effect of the Region 1 currents penetrate to mid and low latitudes. Hermanus in the southern hemisphere observes the magnetopause current, even though it is conjugate to Tihany that observes the Region 1 currents instead. The difference in the response of the magnetosphere to the pressure pulse studied here and more typical SI events can be explained by the strong pre-existing southward IMF that has already stretched and loaded energy into the magnetosphere. Also the fact that the perturbation studied here is a pulse with an extended distinct rise and decay time, as opposed to the SI and SSC events that are step-like changes in the pressure, where the pressure rises fast and remains high for a longer period. As a result we do not observe the initial transient signatures customary in SI events (Araki, 1994).

SUMMARY AND CONCLUSIONS

We have studied the effect of the Jan 10, 1997 dynamic pressure pulse on the magnetospheric currents. The pressure front hits the magnetosphere at 1050 UT and was large enough to engulf and constrict the entire magnetosphere within the 25 minutes of its duration. The response of the magnetosphere was practically instantaneous, global and directly driven by the propagation of the solar wind density enhancement region through the magnetosphere. It started with the onset of the pressure pulse and ended with the end of the pressure pulse. These are not the characteristics of a typical substorm. About 10 minutes before the pressure pulse encountered the magnetosphere an auroral enhancement did occur, likely a substorm onset (Kamide et al., 1998). The arrival of the pressure pulse had the profound effect of strengthening and widening the oval, the auroral electrojet and the Region 1 currents. We interpret this as the driven response of the magnetosphere to the pressure pulse affecting ongoing activity and not as a new substorm onset. The initial compression created a global rapid strengthening of the magnetopause, tail and Region 1 currents. A few minutes later, and by the time the pressure front reached well into the magnetotail, the response was the closing of more flux in the nightside. We believe the effect of the pressure pulse is so profound and global because of the prior extended period of strongly southward IMF that stretched and loaded the magnetosphere with energy. Therefore when the pressure pulse hits, the magnetosphere has been “preconditioned” to respond strongly. This is in agreement with the conclusions of Shue and Kamide [1998]. Li et al. [1998] also report evidence for the “preconditioning” of the magnetosphere. Li et al. observed a rapid enhancement of 0.4 to 1.6 MeV electrons in the magnetosphere at L=4.2-6, immediately following the pressure pulse of Jan 10, 1997. They attributed that enhancement to the pressure pulse quickly energizing a source population of electrons that was present in the magnetosphere from the intense activity during the previous hours.

Finally we found some basic differences between the magnetospheric response to the Jan 10, 1997 pressure pulse and typical SI events. There was no preliminary transient response to the pressure front, as has been reported at the beginning of other SI events (Araki et al., 1994). Most important the dayside magnetometers at mid and sub-auroral latitudes did not observe the positive bay characteristic of the increase in the magnetopause current, instead they observed the effect of the increased Region 1 currents. This was because, under conditions of southward IMF, the strengthening of the Region 1 currents from the compression was so strong that it completely canceled out the effect of the magnetopause current at dayside L-shells as low as 1.5.

Acknowledgements: This work was supported by the National Science Foundation grants OPP-9619733 and ATM98-03431 and NASA grants NAG5-6243 and NAG5-7962. D. Lummerzheim was supported by NASA grant NAG5-7683. We thank Drs K. Ogilvie and R. Lepping of Goddard Space Flight Center for the WIND plasma and magnetic field data, S. Kokubun for the Geotail magnetic field data, L. Frank and B. Patterson of U. of Iowa for the Geotail plasma data, and J. Samson of U. of Alberta for the MSP data. We also thank J. Hughes for the MACCS magnetometer data, the Danish Meteorological Institute for the Greenland data, the Finish Meteorological Institute for the IMAGE data, the Canadian Space agency for the CANOPUS data, the Geological Survey of Canada for their magnetometer data, and Les Morris of the National Geophysical Data Center for providing a useful source of ground magnetometer data from a global network of stations. The first author thanks the NOAA Space Environment Center and the National Research Council for the portion of this work completed at SEC while an NRC Associate.

REFERENCES

Araki, T., Global structure of geomagnetic sudden commencement, *Plan. Space Sci., 25*, 373, 1977.

Araki, T., K. Schlegel, and H. Lühr, Geomagnetic effects of the hall and pedersen current flowing in the auroral ionosphere, *J. Geophys. Res., 94*, 17185, 1989.

Araki, T., A physical model of the geomagnetic sudden commencement, in *the Solar Wind Sources of Magnetospheric Ultra-Low-Frequency Waves* edited by M. J. Engebretson, K. Takahashi, and M. Scholer, 183, 1994.

Blanchard, G. T., L.R, Lyons, and J. C. Samson, Accuracy of 6300 Å auroral emission to identify the separatrix on the night side of the Earth, *J. Geophys. Res., 102*, 9697. 1997.

Burch, J. L., Preconditions for the triggering of polar magnetic substorms by storm sudden commencements, *J. Geophys. Res., 77,* 5629, 1972.

Burgess, D., Collisionless shocks, in *Introduction to Space Physics*, edited by M. G. Kivelson and C. T. Russell, 129-163, Cambridge U. Press, New York, 1995.

Iijima, T., Interplanetary and ground magnetic conditions preceding ssc-trigged substorms, *Rep. Ionos. Space Res. Japan, 27*, 205, 1973.

Kamide, Y., J.-H. Shue, X. Li, G. Lu, M. J. Brittnacher, G. K. Parks, and G. D. Reeves, Internally and externally triggered substorms: a case study of the January 10, 1997 events, in *SUBSTORMS-4* edited by S. Kokubun and Y. Kamide, 305, 1998.

Kaufmann, R. L., and A. Konradi, Explorer 12 magnetopause observations: Large-scale nonuniform motion, *J. Geophys. Res.*, 74, 3609, 1969.

Kokubun, S., R. L. McPherron, and C. T. Russell, Triggering of substorms by solar wind discontinuities, *J. Geophys. Res., 82*, 74, 1977.

Le, G., C. T. Russell, S. M. Petrinec, and M. Ginskey, Effect of sudden solar wind dynamic pressure changes at subauroral latitudes: Change in magnetic field, *J. Geophys. Res., 98*, 3982, 1993.

Li, X., D. N. Baker, M. Temerin, T. Cayton, G. D. Reeves, T. Araki, H. Singer, D. Larson, R. P. Lin, and S. G. Kanekal, Energetic electron injection into the inner magnetosphere during the Jan. 11-11, 1997 magnetic storm, *Geophys. Res. Let., 25*, 2561, 1998.

Lummerzheim, D. and J. Lilensten, Electron Transport and Energy Degradation in the Ionosphere: Evaluation of the Numerical Solution, Comparison with Laboratory Experiments and Auroral observations, *Ann. Geophys., 12*, 1039, 1994.

Russell, C. T., M. Ginskey, and S. M. Petrinec, Sudden impulses at low latitude stations: Steady state response for northward interplanetary magnetic field, *J. Geophys. Res., 99*, 253, 1994a.

Russell, C. T., M. Ginskey, and S. M. Petrinec, Sudden impulses at low latitude stations: Steady state response for southward interplanetary magnetic field, *J. Geophys. Res., 99*, 13403. 1994b.

Russell, C. T., and M. Ginskey, Sudden impulses at subauroral latitudes: Response for northward interplanetary magnetic field, J. Geophys. Res., 100, 23695, 1995.

Shue, J.-H., and Y. Kamide, Effects of solar wind density on the westward electrojet, in *SUBSTORMS-4* edited by S. Kokubun and Y. Kamide, 1998.

Siscoe, G. L., W. Lotko, and B. U. Ö. Sonnerup, A high-latitude boundary layer model of the convection current system, *J. Geophys. Res., 96*, 3487-3495, 1991.

Torr, M. R., D. G. Torr, M. Zukic, R. B. Johnson, J. Ajello, P. Banks, K. Clark, K. Cole, C. Keffer, G. Parks, B. Tsurutani, J. Spann, A far ultraviolet imager for the international solar-terrestrial physics mission, *Space Sci. Rev., 71*, 329, 1995.

FIGURE CAPTIONS

Figure 1. Solar wind plasma and interplanetary magnetic field data from the WIND spacecraft.

Figure 2. Plasma and magnetic field data from Geotail, located in the magnetosheath.

Figure 3. Interpolated equivalent current patterns from a global network of magnetometers.

Figure 4. The H component of the magnetic field from stations at many local times and latitudes >70° on the left panel, between 60° and 70° in the middle panel, and between 50° and 60° in the right panel.

Figure 5. The H component of mid- and low-latitude magnetometers in the 11 to 13 MLT region, panel (a), and from all local times, panel (b).

Plate 1. Top: A series of 25 images of the precipitating particle energy flux, from the POLAR UVI instrument. Bottom: 5577 Å emission line from the Rankin and Gillam meridional scanning photometers.

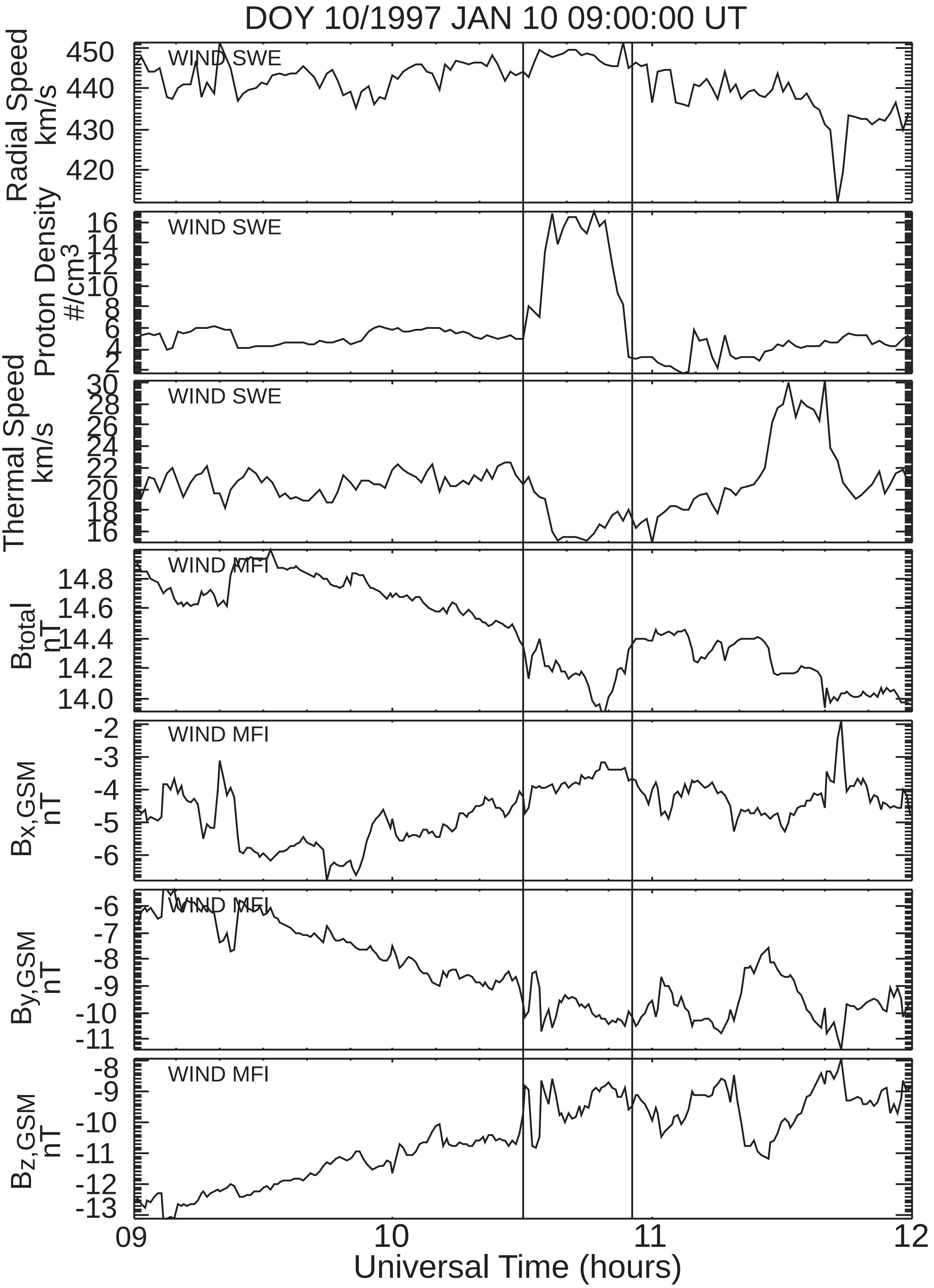
DOY 10/1997 JAN 10 09:00:00 UT
Radial Speed km/s
450
440
430
420
WIND SWE
Proton Density #/cm3
16
14
12
10
8
6
4
2
WIND SWE
Thermal Speed km/s
30
28
26
24
22
20
18
16
WIND SWE
Btotal nT
14.8
14.6
14.4
14.2
14.0
WIND MFI
Bx,GSM nT
-2
-3
-4
-5
-6
WIND MFI
By,GSM nT
-6
-7
-8
-9
-10
-11
WIND MFI
Bz,GSM nT
-8
-9
-10
-11
-12
-13
WIND MFI
09
10
11
12
Universal Time (hours)

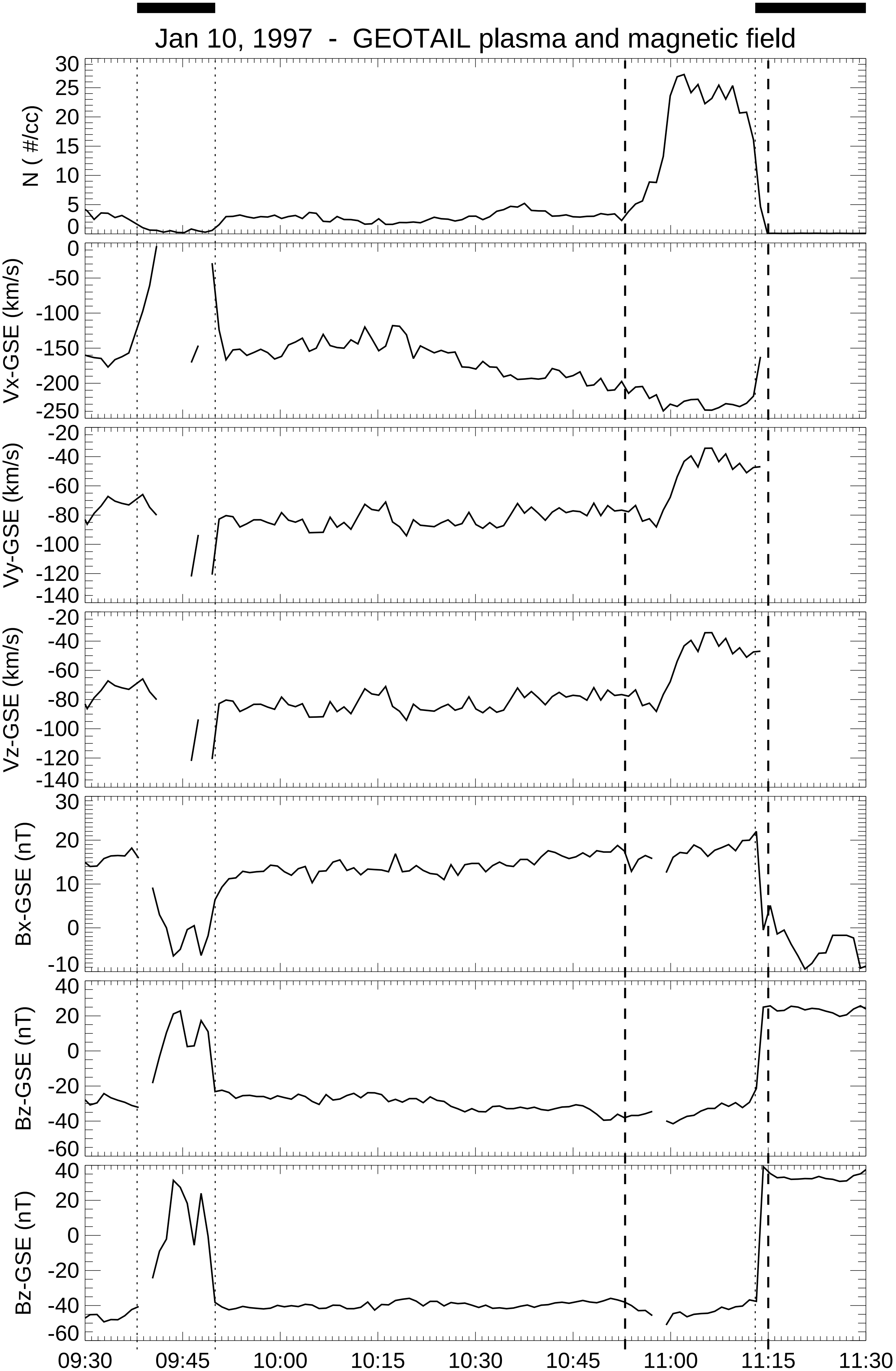
Jan 10, 1997 - GEOTAIL plasma and magnetic field
N (#/cc)
30
25
20
15
10
5
0
Vx-GSE (km/s)
0
-50
-100
-150
-200
-250
Vy-GSE (km/s)
-20
-40
-60
-80
-100
-120
-140
Vz-GSE (km/s)
-20
-40
-60
-80
-100
-120
-140
Bx-GSE (nT)
30
20
10
0
-10
Bz-GSE (nT)
40
20
0
-20
-40
-60
Bz-GSE (nT)
40
20
0
-20
-40
-60
09:30
09:45
10:00
10:15
10:30
10:45
11:00
11:15
11:30

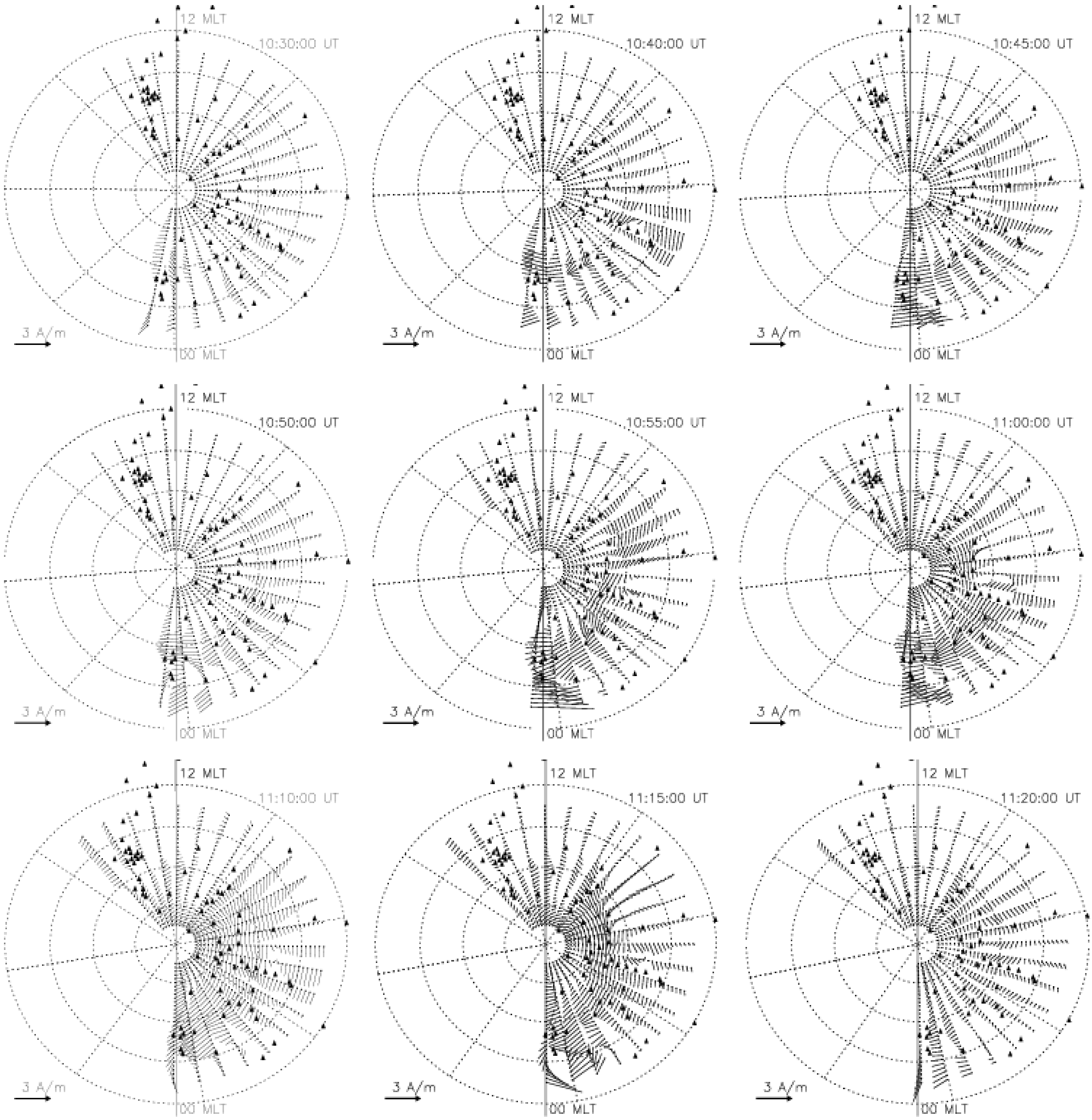
12 MLT
10:30:00 UT
3 A/m
00 MLT
12 MLT
10:40:00 UT
3 A/m
00 MLT
12 MLT
10:45:00 UT
3 A/m
00 MLT
12 MLT
10:50:00 UT
3 A/m
00 MLT
12 MLT
10:55:00 UT
3 A/m
00 MLT
12 MLT
11:00:00 UT
3 A/m
00 MLT
12 MLT
11:10:00 UT
3 A/m
00 MLT
12 MLT
11:15:00 UT
3 A/m
00 MLT
12 MLT
11:20:00 UT
3 A/m
00 MLT

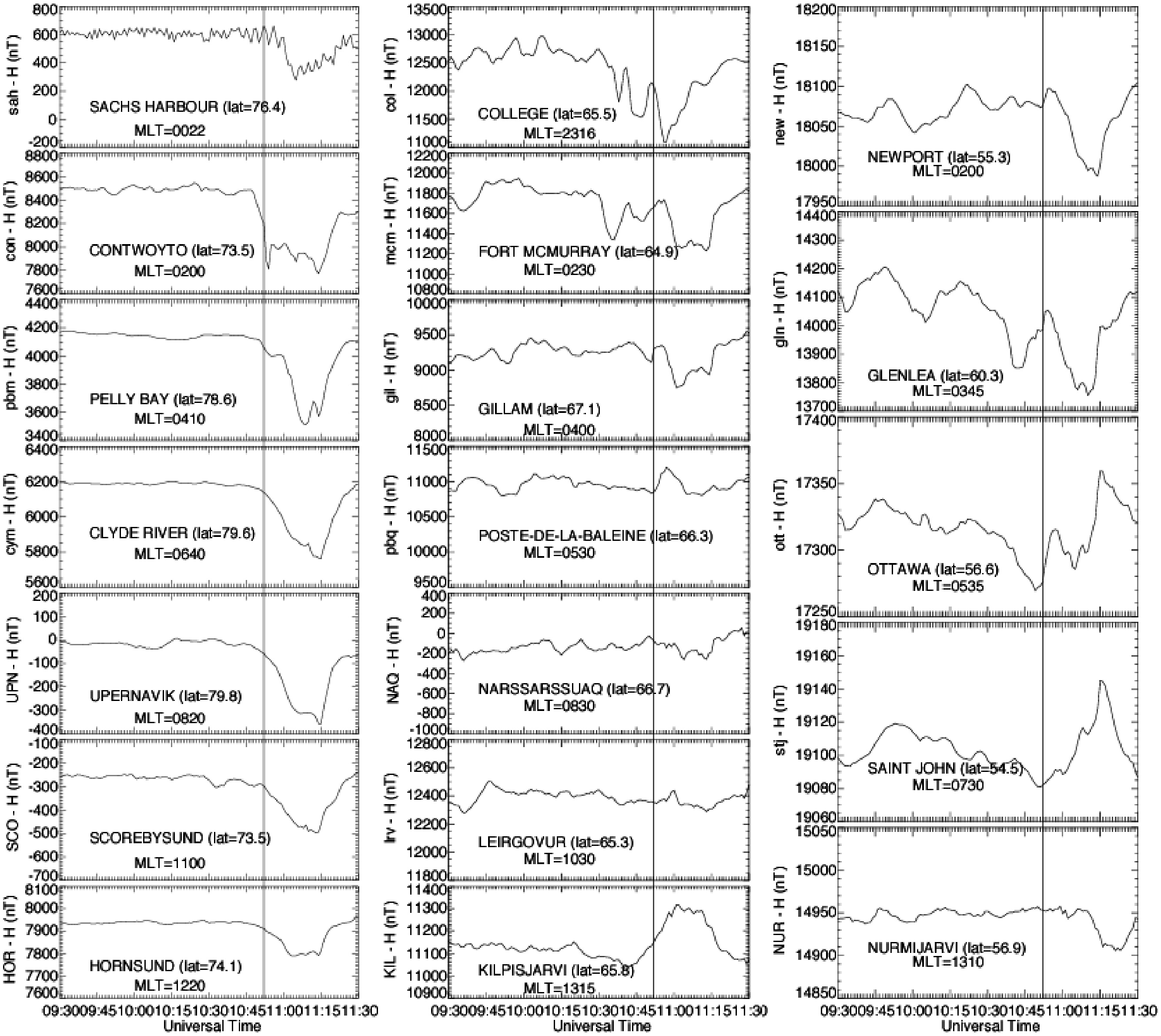
sah - H (nT)
SACHS HARBOUR (lat=76.4)
MLT=0022
con - H (nT)
CONTWOYTO (lat=73.5)
MLT=0200
pbm - H (nT)
PELLY BAY (lat=78.6)
MLT=0410
cym - H (nT)
CLYDE RIVER (lat=79.6)
MLT=0640
UPN - H (nT)
UPERNAVIK (lat=79.8)
MLT=0820
SCO - H (nT)
SCOREBYSUND (lat=73.5)
MLT=1100
HOR - H (nT)
HORNSUND (lat=74.1)
MLT=1220
col - H (nT)
COLLEGE (lat=65.5)
MLT=2316
mcm - H (nT)
FORT MCMURRAY (lat=64.9)
MLT=0230
gil - H (nT)
GILLAM (lat=67.1)
MLT=0400
pbq - H (nT)
POSTE-DE-LA-BALEINE (lat=66.3)
MLT=0530
NAQ - H (nT)
NARSSARSSUAQ (lat=66.7)
MLT=0830
lrv - H (nT)
LEIRGOVUR (lat=65.3)
MLT=1030
KIL - H (nT)
KILPISJARVI (lat=65.8)
MLT=1315
new - H (nT)
NEWPORT (lat=55.3)
MLT=0200
gln - H (nT)
GLENLEA (lat=60.3)
MLT=0345
ott - H (nT)
OTTAWA (lat=56.6)
MLT=0535
stj - H (nT)
SAINT JOHN (lat=54.5)
MLT=0730
NUR - H (nT)
NURMIJARVI (lat=56.9)
MLT=1310
09:30 09:45 10:00 10:15 10:30 10:45 11:00 11:15 11:30
Universal Time

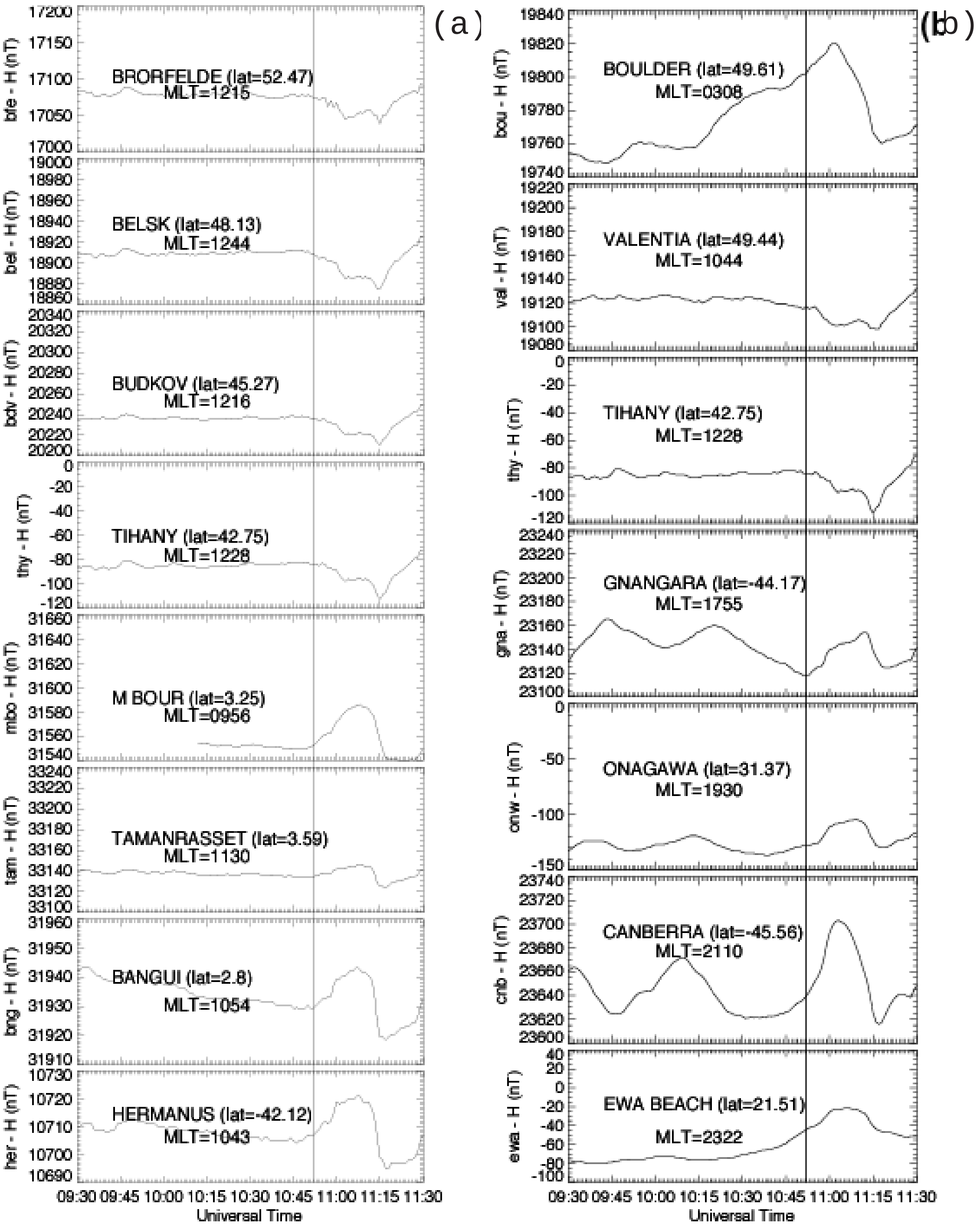
(a)
BRORFELDE (lat=52.47) MLT=1215
bfe - H (nT)
BELSK (lat=48.13) MLT=1244
bel - H (nT)
BUDKOV (lat=45.27) MLT=1216
bdv - H (nT)
TIHANY (lat=42.75) MLT=1228
thy - H (nT)
M BOUR (lat=3.25) MLT=0956
mbo - H (nT)
TAMANRASSET (lat=3.59) MLT=1130
tam - H (nT)
BANGUI (lat=2.8) MLT=1054
bng - H (nT)
HERMANUS (lat=-42.12) MLT=1043
her - H (nT)
09:30 09:45 10:00 10:15 10:30 10:45 11:00 11:15 11:30
Universal Time
(b)
BOULDER (lat=49.61) MLT=0308
bou - H (nT)
VALENTIA (lat=49.44) MLT=1044
val - H (nT)
TIHANY (lat=42.75) MLT=1228
thy - H (nT)
GNANGARA (lat=-44.17) MLT=1755
gna - H (nT)
ONAGAWA (lat=31.37) MLT=1930
onw - H (nT)
CANBERRA (lat=-45.56) MLT=2110
cnb - H (nT)
EWA BEACH (lat=21.51) MLT=2322
ewa - H (nT)
09:30 09:45 10:00 10:15 10:30 10:45 11:00 11:15 11:30
Universal Time

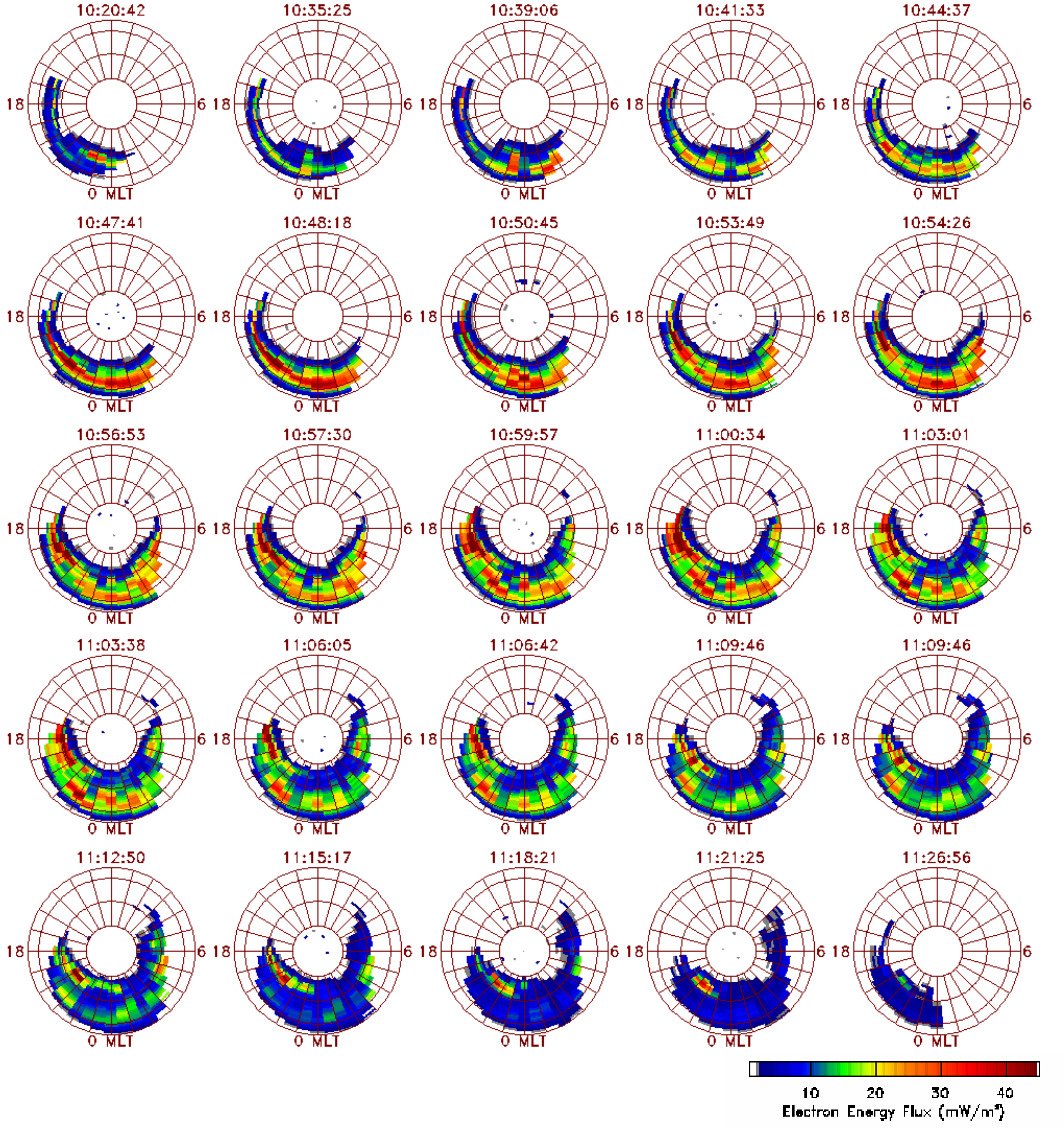
10:20:42
10:35:25
10:39:06
10:41:33
10:44:37
10:47:41
10:48:18
10:50:45
10:53:49
10:54:26
10:56:53
10:57:30
10:59:57
11:00:34
11:03:01
11:03:38
11:06:05
11:06:42
11:09:46
11:09:46
11:12:50
11:15:17
11:18:21
11:21:25
11:26:56
18
6
0 MLT
10
20
30
40
Electron Energy Flux (mW/m²)

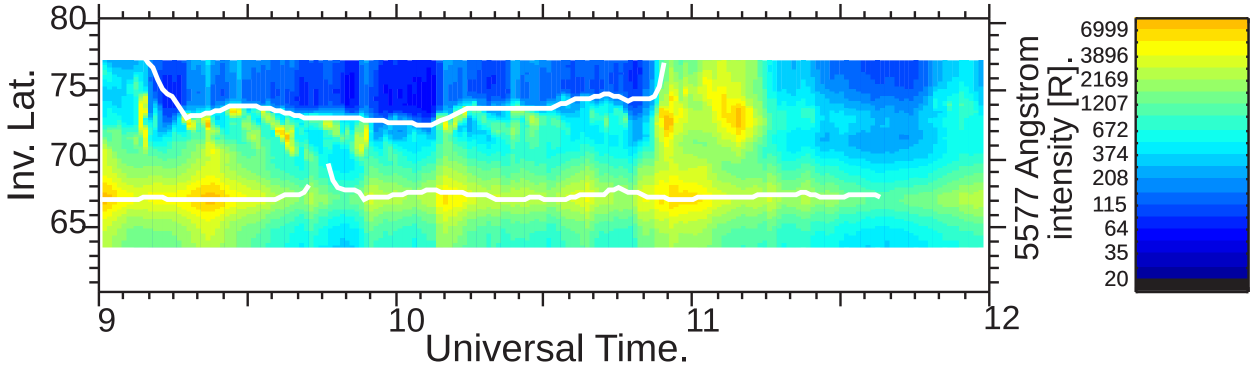
80
75
70
65
Inv. Lat.
9
10
11
12
Universal Time.
5577 Angstrom intensity [R].
6999
3896
2169
1207
672
374
208
115
64
35
20